Title

Dissolution and Aggregation of Metal Oxide Nanoparticles in Root Exudates and Soil Leachate: Implications for Nanoagrochemical Application.

Journal

Environmental science & technology, 55(20)

ISSN

0013-936X

Authors

Cervantes-Avilés, Pabel
Huang, Xiangning
Keller, Arturo A

Publication Date

2021-10-01

DOI

10.1021/acs.est.1c00767

Peer reviewed

Environmental Science & Technology

pubs.acs.org/est

Article

Dissolution and Aggregation of Metal Oxide Nanoparticles in Root Exudates and Soil Leachate: Implications for Nanoagrochemical Application

Pabel Cervantes-Avilés, Xiangning Huang, and Arturo A. Keller*

Cite This: https://doi.org/10.1021/acs.est.1c00767

Read Online

ACCESS | Metrics & More | Article Recommendations | Supporting Information

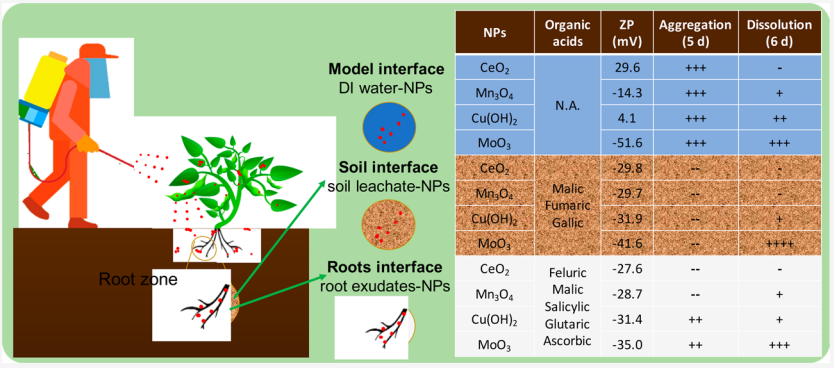

NPs	Organic acids	ZP (mV)	Aggregation (5 d)	Dissolution (6 d)
CeO_2	N.A.	29.6	+++	-
Mn_3O_4		-14.3	+++	+
$Cu(OH)_2$		4.1	+++	++
MoO_3		-51.6	+++	+++
CeO_2	Malic Fumaric Gallic	-29.8	--	-
Mn_3O_4		-29.7	--	-
$Cu(OH)_2$		-31.9	--	+
MoO_3		-41.6	--	++++
CeO_2	Feluric Malic Salicylic Glutaric Ascorbic	-27.6	--	-
Mn_3O_4		-28.7	--	+
$Cu(OH)_2$		-31.4	++	+
MoO_3		-35.0	++	+++

ABSTRACT: Knowledge of dissolution, aggregation, and stability of nanoagrochemicals in root exudates (RE) and soil leachate will contribute to improving delivery mechanisms, transport in plants, and bioavailability. We characterized aggregation, stability, and dissolution of four nanoparticles (NPs) in soybean RE and soil leachate: nano-CeO_2, nano-Mn_3O_4, nano-$Cu(OH)_2$, and nano-MoO_3. Aggregation differed considerably in different media. In RE, nano-$Cu(OH)_2$, and nano-MoO_3 increased their aggregate size for 5 days; their mean sizes increased from 518 ± 43 nm to 938 ± 32 nm, and from 372 ± 14 nm to 690 ± 65 nm, respectively. Conversely, nano-CeO_2 and nano-Mn_3O_4 disaggregated in RE with time, decreasing from 289 ± 5 nm to 129 ± 10 nm, and from 761 ± 58 nm to 143 ± 18 nm, respectively. Organic acids in RE and soil leachate can be adsorbed onto particle surfaces, influencing aggregation. Charge of the four NPs was negative in contact with RE and soil leachate, due to organic matter present in RE and soil leachate. Dissolution in RE after 6 days was 38%, 1.2%, 0.5%, and <0.1% of the elemental content of MoO_3, $Cu(OH)_2$, Mn_3O_4, and CeO_2 NPs. Thus, the bioavailability and efficiency of delivery of the NPs or their active ingredients will be substantially modified soon after they are in contact with RE or soil leachate.

KEYWORDS: *nanofertilizers, nanopesticides, nanoenabled agricultural products, single particle ICP-MS, size distribution*

INTRODUCTION

Nanotechnology is generating new products and applications in many fields such as medicine, food sciences, electronics, environmental sciences, agriculture, among others.[1] In agriculture, nanotechnology aims to make it more efficient, resilient, and sustainable.[2] Currently, nanomaterials (NMs) may contribute to monitor crops,[3] improve the growth of food plants,[4] enhance their nutritional quality,[5] control agricultural pests,[6] and regulate metabolic processes of crop species.[7] However, it is important to understand the modifications that occur to NMs and that can affect the delivery of the NMs or their active ingredients to the target plant when NMs are applied.

NMs applied as nanofertilizers or nanopesticides are part of a new generation of agrochemicals, namely nanoenabled agricultural products.[8,9] The delivery systems for these nanoenabled agricultural products often employ conventional methods, applied directly to soil or hydroponic medium, foliar application, or seed priming/coating.[5] Although the majority of NMs applied via leaves and soil do not enter the plant, some of the NMs are trapped in the epidermis and some others are transported effectively into the plant tissues.[10] When NMs are added directly to soil, their transport and interactions with the roots are influenced by the type of NMs, soil composition, pore size of the pit membrane, and properties of the xylem/phloem such as sap composition and sap flow rate.[5,10,11]

Special Issue: Environmental Implications of Nanofertilizers

Received: February 3, 2021
Revised: May 11, 2021
Accepted: May 12, 2021

However, understanding how root exudates (RE) affect and influence NM transport and fate is crucial for the design and improvement of root−NMs interactions.[12,13] Therefore, there is a need to better understanding the aggregation, stability, and dissolution of NMs used as nanoagrochemicals, which influence their transport, bioavailability, as well as the interactions with plant-derived biomolecules.[14]

In the past few years, there has been an increasing use of nanofertilizers and nanopesticides based on metal oxides.[11] In particular, nano-CeO_2 pesticides and Cu-based (oxides and hydroxides) nanomaterials have been applied as nanopesticides or nanofertilizers in experimental studies.[5,11] The properties of these NMs influence their behavior, for example, positively charged nano-CeO_2 had more affinity to the roots of tomato plants, while negatively charged nano-CeO_2 had better transport ability.[15] In addition, the soil organic matter content promoted the mobility of the nano-CeO_2 into the roots of corn plants exposed from 100 to 800 mg/kg of soil.[16] Cu-based NMs have also presented mobility from roots to shoots via xylem in Maize (*Zea mays L.*) exposed to 10 and 100 mg/L of nano-CuO;[17] This experiment also indicated the affinity between nano-CuO and the RE. Similarly, Huang et al., (2017) reported that synthetic RE and its components highly influence the dissolution, transformation and aggregation of Cu-based nanomaterials.[14] The actual charge of the NMs and their stability in the roots and surrounding media (e.g., RE) influence their fate and effect on plants.[18,19] Hence, these properties should be evaluated in realistic media such as natural RE and soil leachate.

Although molybdenum is a micronutrient for plants,[5] the application of nano-MoO_3 (via foliar or soil) as micronutrient and/or promotor of plant growth have been limited.[7,20,21] Osman et al. (2020) reported that nano-MoO_3 as foliar micronutrient decreased the quality and quantity of dry bean plants, but increased the productivity of common bean plants compared to molybdenum salt at (10−40 mg/L).[20] Conversely, a combination of microbial preparation and a colloidal suspension of molybdenum nanoparticles applied via soil at 8 mg/L to a *Cicer arietinum* L. stimulated the nodule formation per plant by four times.[21] Manganese is also a micronutrient used in acidic soil,[22] but its use as nano-Mn_3O_4 has been limited. Recently, nano-Mn_3O_4 was applied to leaves by spraying a suspension of 20 mg/L, after 20 days from the sowing of the seeds of squash plants until 40 days from sowing,[23] improving the growth plant yield but decreasing the yield of fruit. Another study reported that nano-Mn_2O_3 applied at 6 mg/kg/plant promoted nutrient fixation in wheat, but it was found that manganese could affect plants in subtle ways when applied in soil rather than via foliar.[24] Although effects have been noted when these NMs are applied in the soil, the mechanisms related to the effect and transport of nano-MoO_3 and nano-Mn_3O_4 in RE have not been studied in detail. Therefore, studies about aggregation and dissolution of nano-MoO_3 and nano-Mn_3O_4 in RE can contribute to understand the interactions between NMs and roots.

In this work, we characterized and determined the aggregation, stability and dissolution, in soybean (*Glycine max*) root exudates, of four nanoparticles (NPs) proposed to be used as nanofertilizers or nanopesticides: nano-CeO_2, nano-Mn_3O_4, nano-$Cu(OH)_2$ and nano-MoO_3. We also studied the early aggregation of these NPs in RE via single particle inductively coupled plasma mass spectrometry (spICP-MS). This study also aimed to determine whether the use of these nanoenabled agricultural products may result in the environmental buildup of metal ions or nanoparticles in the roots-soil interface.

MATERIALS AND METHODS

Nanoparticles. Four bare metal oxide nanoparticles (NPs), CeO_2, $Cu(OH)_2$, MoO_3, and Mn_3O_4, were used for these experiments because they have been proposed to be incorporated in agricultural products. CeO_2 NPs were received from Meliorum Technologies (U.S.), and $Cu(OH)_2$, MoO_3, and Mn_3O_4NPs were acquired from U.S. Research Nanomaterials Inc. (U.S.). Stock suspensions were prepared, consisting of 1000 mg of NPs in 1 L of NANOpure water (Thermo Scientific Barnstead) with a specific resistance of 18.2 MΩ-cm. A 50 mg/L suspension of Au NPs in 2 mM sodium citrate and with nominal size of 60 nm was purchased from Nano-Composix Inc. and used as reference material in spICP-MS measurements.

Characterization of Metal Nanoparticles. Characterization consisted of determining the morphology, size, localized surface plasmon resonance (LSPR), surface composition, phase, and crystalline structure of the NPs. To determine the morphology and primary size, transmission electron microscopy (TEM) was used (Jeol 1230 EM and FEI Tecnai G2). Size distribution and zeta potential (ZP) in different suspensions was determined by laser Doppler velocimetry (Zetasizer Nano ZS90, Malvern Panalytical). LSPR was determined by the UV spectrophotometer (Shimadzu, UV 1800). Surface composition and purity was determined by X-ray photoelectron spectrometry (XPS, Thermo Scientific, ESCALAB 250 XI^+). Phase and crystalline structure were determined by comparing the X-ray diffraction (XRD) spectrum obtained (Panalytical Empyrean Powder) with the patterns in the database. Specific surface areas were provided by the manufacturers for all NPs.

Soybean RE. Pregerminated seedlings were grown in vermiculite in glass jars until the full expansion of the first true leaf (10−12 days). Then, the plants were transplanted to vermiculite in culture boxes. Hoagland nutrient solution at 10% was supplemented to the plants every alternate day. Pregermination and culturing occurred at 20 °C in an environmental growth chamber with a 16 h photoperiod. After 28−30 days of culturing, the soybean seedlings were removed from the culture box, and the roots were washed thoroughly with NANOpure water for RE collection. The procedure for collection of RE was modified from the protocol described by Zhao et al. (2016).[25] Briefly, the seedlings were placed for 12 h in new metal free tubes containing 40 mL of autoclaved 0.1 mM $CaCl_2$ as the solution to collect RE. This solution was aerated continuously during the 12 h period of collection. After 12 h, the 0.1 mM $CaCl_2$ solution with secreted metabolites was filtered using a syringe filter (0.45 μm) to remove larger particles and microorganisms. The filtrate was used for the NP dissolution and aggregation experiments. Analysis of the soybean RE composition was performed in triplicate via liquid chromatography coupled to triple quadrupole mass spectrometry (LC-MS/MS), based on the methods developed in previous studies.[26]

Soil Leachate Extraction. Vermiculite soil with pH 7.4, EC 880 μS/cm, cation exchange capacity (CEC) 120 cmol/kg and <0.8% of organic matter was used in the experiments. The standard method ASTM D 3987 was used to extract the water-soluble compounds from the vermiculite soil. The procedure

https://doi.org/10.1021/acs.est.1c00767
Environ. Sci. Technol. XXXX, XXX, XXX−XXX

Table 1. Summary of the Characterization of Metal Oxide Nanoparticles in DI water, RE, and Soil Leachate

	CeO_2	$Cu(OH)_2$	MoO_3	Mn_3O_4
Dissolved Ions Released From NPs after 6 Days in				
DI water (pH 6.5)	<0.01 mg/L	16.4 mg/L	38.9 mg/L	2.5 mg/L
root exudates (pH 6.8)	<0.01 mg/L	1.2 mg/L	38.0 mg/L	0.3 mg/L
soil leachate (pH 7.4)	<0.01 mg/l	0.12 mg/l	55.9 mg/l	0.6 mg/l
crystalline structure	cubic, ceria	orthorhombic	orthorhombic, α-moo$_3$	tetragonal, hausmannite
binding energy region, main peaks	Ce 3d, 883 eV	Cu 2p, 933.5 eV	Mo 3d, 230.9 eV	Mn 2p, 642.7 eV
shape	nanorods	nanorods-nanowires	nanoparticles (mainly spheres)	nanoparticles (mainly spheres)
primary size(ø: diameter)	ø: 8 nm, length: 67 nm	ø: 50 nm, length: 2−5 μm	ø: 13−80 nm	ø: 30−60 nm
Zeta Potential in				
DI water	29.6 ± 0.4 mV	4.1 ± 2.4 mV	−51.6 ± 1.1 mV	−14.3 ± 0.7 mV
root exudates	−27.6 ± 0.8 mV	−31.4 ± 0.6 mV	−35.0 ± 1.2 mV	−28.7 ± 0.9 mV
soil leachate	−29.8 ± 0.9 mV	−31.9 ± 1.8 mV	−41.6 ± 0.6 mV	−29.7 ± 1.2 mV
Aggregate Size after 5 Days in				
DI water	298.9 ± 28.8 nm	1489.9 ± 231.6 nm	606.8 ± 69.6 nm	5919.0 ± 696.5 nm
root exudates	129.3 ± 10.2 nm	938.2 ± 32.3 nm	690.1 ± 65.1 nm	146.3 ± 17.9 nm
soil leachate	129.5 ± 8.1 nm	356.2 ± 41.1 nm	221.1 ± 30.1 nm	135.5 ± 12.4 nm
purity (TGA)	95.14%	99.50%	≥99.94%	99.95%
specific surface area (BET)	93.8 m^2/g	14 m^2/g	65m^2/g	65m^2/g
localized surface plasmon resonance	311 nm	293 nm	291 nm	511 nm

consisted in weighting 4 g vermiculite soil and placing it in a metal free tube. NANOpure water was added at a ratio of 1:1 (v/v) of leachate/soil and then the suspension was mixed for 1 h of vortex at 3000 rpm. Then the slurry was centrifuged 20 min at 5000 rpm and 20 °C; then, slurry was filtered to remove particles larger than 0.45 μm. The filtrate was collected and analyzed in triplicate for screening of organic acids by LC-MS/MS.

Aggregation Studies. The aggregation and stability experiments consisted of 12 treatments: four types of NP ($Cu(OH)_2$, Mn_3O_4, MoO_3, and CeO_2) and three media (NANOpure water, soybean RE, and soil leachate). All 12 treatments were performed per triplicate following ANOVA one factor for each treatment. A concentration of 100 mg/L as metal content of each NP ($Cu(OH)_2$, Mn_3O_4, MoO_3 and CeO_2) was spiked separately in 50 mL metal-free polypropylene tubes containing either water, RE or soil leachate. This concentration is in the range used in studies testing NPs by foliar spray or added to soils (1−2000 mg/L, 1−100 mg/plant, or 100−800 mg/kg of soil).[7] Tubes were sonicated 20 min after spiking the NPs and left to stand for 5 days. Samples were collected immediately after sonication period, and at days 1, 3, and 5 for aggregate size measurements (Zetasizer Nano ZS90). Aggregate size was determined per triplicate and reported values correspond to the average of 10 readings per replicate. The size distribution during the first 6 h was also determined using spICP-MS, as described below. The charge of all four NPs in water, RE and soil leachate was evaluated by measuring the zeta potential after 5 days in triplicate (Zetasizer Nano ZS90). Each value corresponded to the average of 10 readings.

Dissolution of NPs. NANOpure, RE, and soil leachate were used in the NP dissolution experiments. 100 mg/L as metal content of each NP was spiked separately in three sets of 50 mL metal-free polypropylene tubes: one for RE, one for soil leachate and another for DI water. The tubes were sonicated 20 min after spiking and left to stand for 6 days. Samples were collected every 24 h, approximately. At sampling time, the tubes were vortexed, and aliquots of 1 mL were transferred to centrifuge tubes. The particles were separated from the supernatant by filtering using Amicon Ultra 3 kDa MWCO tubes. Filtered aqueous media was diluted with HNO_3 3% for regular ICP-MS analysis. Ionic determination analyses were performed in three replicates, and the mean concentration corresponds to the average of replicates.

Determination of the Size Distribution via Single Particle ICP-MS (spICP-MS). The size distribution of NPs during the first 6 h of exposure to RE was determined via spICP-MS. The instrument was an Agilent 7900 ICP-MS (Santa Clara, CA) with the spICP-MS module. The instrument was equipped with an autosampler and a standard peristaltic pump, standard glass concentric nebulizer, quartz spray chamber and quartz torch, standard nickel sampling and skimmer cones. Analyses were performed in time-resolved analysis (TRA) mode using an integration time (dwell time) of 100 μs per point with no settling time between measurements, similar to a previous study.[27] The instrument settings used for the spICP-MS analysis are summarized in Supporting Information (SI) Table S1.

Calibration of the spICP-MS for NPs quantification was done by tuning the particle size of a reference material (Au NP 60 nm in 2 mM sodium citrate, NanoComposix Inc.) and determining the elemental response factor for the reference material and analyzed elements. The 60 nm Au NP reference standard was diluted to 100 ng/L with DI to determine the nebulization efficiency (η_n). η_n is also known as transport efficiency and this is used for data conversion from raw signal to NP size. The nebulization efficiency was 5.4%, calculated based on the particle size method.[28,29] NP size was calculated from the mass of the particle,[29,30] considering the densities and mass fractions provided by the manufacturers (SI Table S1), and assuming the NPs are spherical.[31] The standard solution containing 10 mg/L of each analyte (Mn, Cu, Mo and Ce) was diluted from 0 to 1 μg/L with 1% wt. HNO_3, to be used to determine the elemental response factor. The samples were diluted with NANOpure water to ensure NP concentration

https://doi.org/10.1021/acs.est.1c00767
Environ. Sci. Technol. XXXX, XXX, XXX−XXX

was between 10 and 100 ng/L. Before dilution of the samples, and again prior to their spICP-MS analyses, all suspensions were placed in an ultrasonic bath for 10 min at 280 W and a frequency of 40 kHz to ensure that the samples were fully homogenized. The spICP-MS analyses were carried out in triplicate, and the results of size distribution were the average of the replicates.

RESULTS AND DISCUSSION

Characterization of Metal Oxide Nanoparticles. The main characteristics of the NPs considered in this study are presented in Table 1. Plots are presented in the Supporting Information. The morphology and primary size of NPs were different but all in the nanoscale (Figure 1). As can be

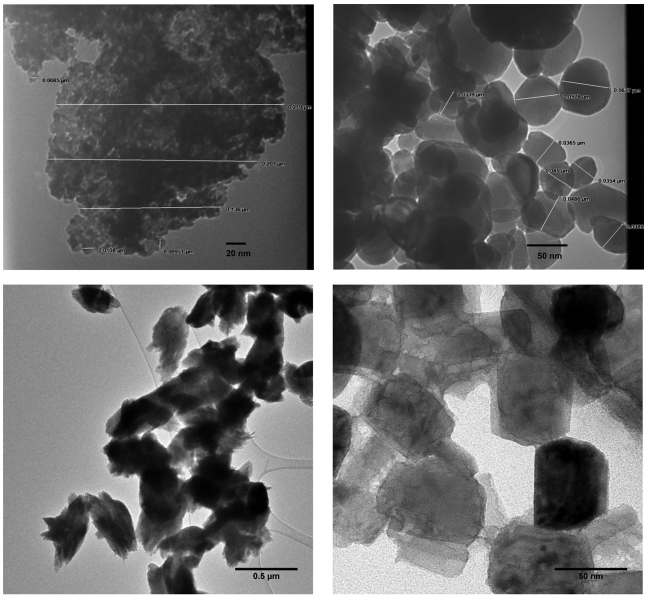

Figure 1. TEM imaging of metal oxide nanoparticles: CeO_2 (top-left), Mn_3O_4 (top-right), $Cu(OH)_2$ (bottom-left) and MoO_3 (bottom-right).

observed, Mn_3O_4 and MoO_3 NPs were generally spherical. CeO_2 and $Cu(OH)_2$ NPs were mostly nanorods and nanobars. Although aggregates were observed for all NPs, the primary size of NPs, for example, diameter, was smaller than 60−70 nm. The nanorods of CeO_2 and $Cu(OH)_2$ had mean diameters of 8 and 50 nm respectively, while the average diameters of Mn_3O_4 and MoO_3 nanospheres were roughly 40 and 60 nm.

Determination of the LSPR helps to understand the photocatalytic activity of NPs. For NPs of CeO_2, $Cu(OH)_2$, and MoO_3, the surface plasmon resonance peaks were localized in the ultraviolet B region at 311, 293, and 291 nm, respectively (SI Figure S1). For Mn_3O_4, the LSPR was in the visible region with a peak at 511 nm, where photocatalytic activity of this material can occur.

The XPS spectra of the four NPs are presented in SI Figures S2 and S3. In the four graphs, a strong peak is observed at 529−530 eV, which corresponds to O 1s and this indicates that oxygen ions associated with an oxidation state 2^- are bound to transition metals,[32] such as those used in our experiments. For CeO_2 NPs, a primary peak for Ce 3d was observed at 883 eV, confirming the presence of Ce (IV) in the binding energy Ce $3d_{5/2}$.[33] The primary peaks observed for Mn_3O_4 NPs were in the region Mn $2p_{3/2}$, with binding energy that corresponds to the presence of MnO and Mn_2O_3 (642.7 eV) and whose oxidation states are Mn (II) and (III).[34] For $Cu(OH)_2$ NPs, the binding energy was measured in the region Cu $2p_{3/2}$ at 933.5 eV and corresponds to Cu (II).[35] In the case of MoO_3 NPs, the primary peak was observed in the region Mo $3d_{3/2}$ at 233 eV and correlates with the oxidation state Mo (VI).[36] The binding energies of these materials indicated they are bound to oxygen in the upper energy levels, and to hydroxide in the case of $Cu(OH)_2$ NPs. Moreover, there were no carbon-based coatings added to the NPs used in the experiments since there were no peaks in the small region 284−288 eV (C 1s binding energy) in all four NPs.

Based on the XRD analyses (SI Figure S4), $Cu(OH)_2$ and MoO_3 exhibited orthorhombic crystalline structure, and MoO_3NPs were associated with the mineral phase alpha (α). For CeO2 NPs, the XRD spectra shows strong peaks at (111), (220) and (311) that are consistent with literature for a cubic crystalline structure,[37] in the well-known phase of ceria. Lastly, the XRD pattern of Mn_3O_4 was associated with a tetragonal structure in databases and corresponds to hausmannite phase. This phase is known to have manganese as Mn^{2+} and Mn^{3+}, which was confirmed in the XPS analysis, and to be a paramagnetic mineral.[38]

Modulation of NM Charge by RE and Soil Leachate. In simple suspensions with DI water at pH 6.5, CeO_2 NPs are positively charged, Mn_3O_4 NPs are negatively charged but less than −20 mV, and the MoO_3 NPs have ZP values between −40 and −60 mV, which imparts significant stability (Figure 2). The $Cu(OH)_2$ nanowires are near their isoelectric point.

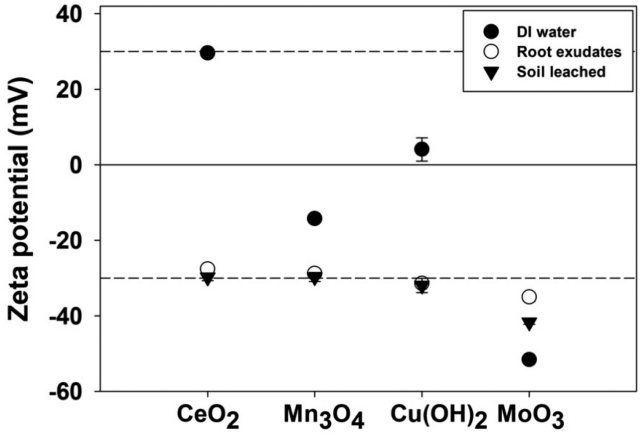

Figure 2. Zeta potential of metal oxide nanoparticles: CeO_2, Mn_3O_4, $Cu(OH)_2$, and MoO_3 in the presence of DI water, RE, and soil leachate. Dash line inside the plot represents ±30 mV considered as stable region for colloids. Error bars represent ± standard deviation of triplicate samples (n = 3).

However, in contact with RE and soil leachate the charge is generally negative for these NPs. Moreover, the charge of all four NPs when exposed to RE and soil leachate was almost independent of NM composition. In RE, the charge was from −28.8 mV to -34.2 mV at the pH of 6.8. In soil leachate (pH 7.4), the charged ranged between −30.5 mV and −42.1 mV. The charge in the surface has been related to the electrolytes and organic molecules present in the media.[16,39] Hence, detailed analysis of electrolytes and composition of organic matter in soil and exudates of agricultural setting will contribute to better understanding of the final charge of nanoenabled products.

https://doi.org/10.1021/acs.est.1c00767
Environ. Sci. Technol. XXXX, XXX, XXX−XXX

Soil leachate and soybean RE were analyzed for organic acids. From a total of 15 organic acids analyzed, only 3 were found in the soil leachate and 5 in the RE (Table 2). Malic acid

Table 2. Concentration of Organic Acids Present in the Soil Leachate and the Soybean RE[a]

	soil leachate		soybean RE	
	mean (μg/L)	SD (μg/L)	mean (μg/L)	SD (μg/L)
fumaric acid	23.71	0.89		
gallic acid	6.23	1.06		
malic acid	104.10	3.46	51.96	8.36
ascorbic acid			998.14	34.99
ferulic acid			18.38	1.23
glutaric acid			298.68	16.71
salicylic acid			147.68	12.20

[a]Mean and standard deviation (SD) of three measurements.

(104.1 μg/L) was the most abundant in the soil leachate, with lower concentration of fumaric acid (23.71 μg/L) and gallic acid (6.23 μg/L). In the case of soybean RE, ascorbic acid (998.1 μg/L) had the highest concentration, followed by glutaric (298.68 μg/L), salicylic (147.68 μg/L), malic (51.96 μg/L), and ferulic (18.38 μg/L) acids. The concentration of these organic acids was low compared to the concentration of the NPs. The positive charge of metal NPs can be neutralized by trace amounts of organic acids in suspensions with pH lower than 8,[40] as we observed for CeO_2 and $Cu(OH)_2$ NPs; while the charge of Mn_3O_4 and MoO_3 NPs did not change substantially (Figure 2). The charge of the CeO_2 and $Cu(OH)_2$ NPs became more negative than the point of zero charge (PZC), which can be due to the presence of other organic ligands not analyzed such as humic acids and amino acids, among others. Since these organic ligands have a negative charge at pH range of 6−8,[35,40] their presence in both media, soil leachate and RE, may contribute to maintaining Mn_3O_4 and MoO_3 NPs negatively charged. The modulation of the charge of the NPs due to the presence of organic ligands in soil and in the roots zone can increase the mobility and the dissolution of metal based NPs;[41,42] hence, further research is needed for systematic evaluation of low molecular weight organic acids and amino acids influence the mobility and transformations of NPs in the root-soil interface.

Aggregation State of Metal Oxide Nanoparticles in RE and Soil Leachate. All four NPs aggregate in DI water with time (Figure 3A), as noted from the first few hours, although there were clear differences at initial state of aggregation. This was expected for Mn_3O_4 and $Cu(OH)_2$ given their ZP close to PZC at the experimental pH, which indicates weak electrostatic repulsions between particles and leading to the aggregation; but unexpected for CeO_2 and MoO_3 NPs given their larger positive and negative ZP, respectively. For these cases, although CeO_2 and MoO_3 NPs form smaller aggregates and generally aggregate at a slower rate, the relatively high concentration of both NPs (100 mg/L) may explain their aggregation over time. Since aggregation behavior is concentration-dependent, these results may be different if the studies are performed at much lower or higher concentrations. The concentrations employed in this study are within the range expected to be used in nanoagrochemical applications. After the aggregation experiments it became clear that 5 days were sufficiently long for colloidal systems containing $Cu(OH)_2$, CeO_2 and MoO_3 NPs to became stable;

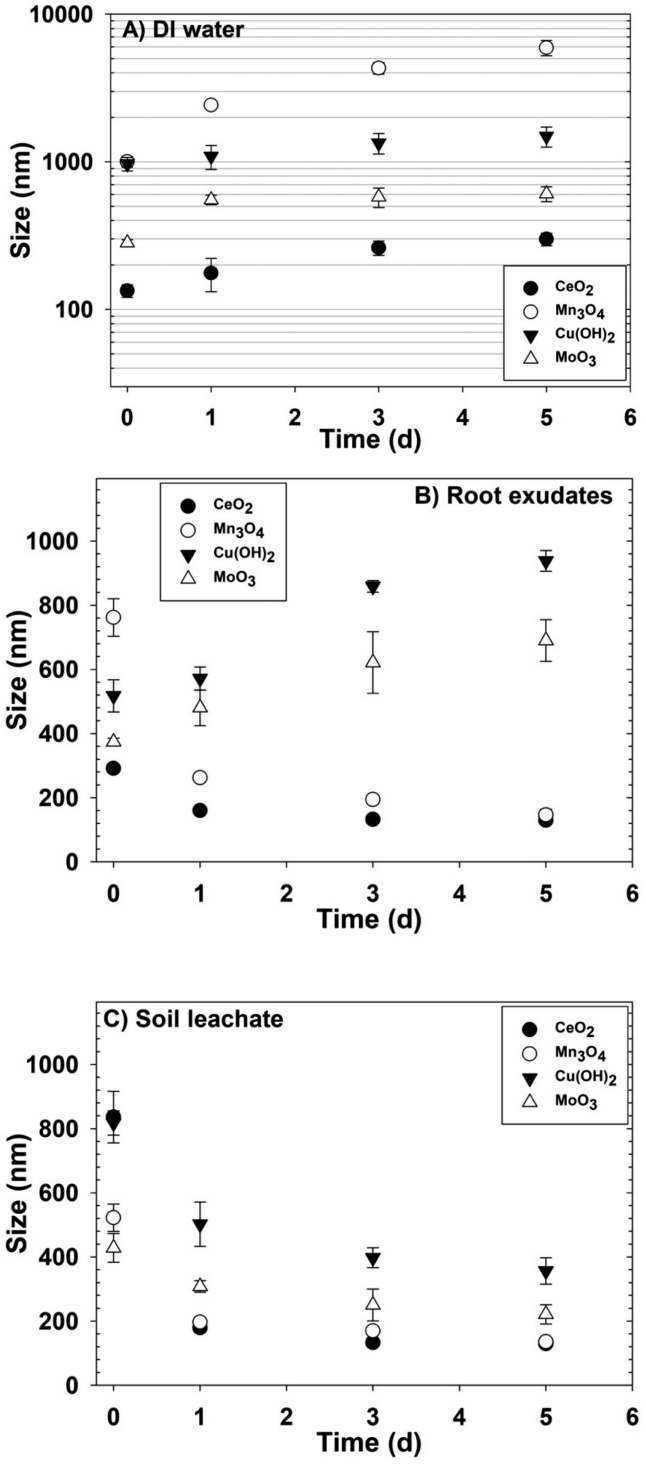

Figure 3. Changes in the aggregate sizes of metal oxide nanoparticles: CeO_2, Mn_3O_4, $Cu(OH)_2$ and MoO_3 during 5 days in (A) DI water: (B) RE; and (C) soil leachate. Error bars represent ± standard deviation of triplicate samples (n = 3).

however, the system containing Mn_3O_4NPs could require more time to reach colloidal stability due to aggregation seems to be ongoing along 5 days. From a nanoagrochemical application, the relatively fast aggregation of these bare NPs could result in significant deposition of the particles, and less bioavailability.

https://doi.org/10.1021/acs.est.1c00767
Environ. Sci. Technol. XXXX, XXX, XXX−XXX

The aggregation of NPs exposed to RE varied significantly (Figure 3B). For $Cu(OH)_2$ and MoO_3 NPs, the aggregate size increased over the 5 days, albeit at different rates, from 518 ± 43 nm to 938 ± 32 nm, and from 372 ± 14 nm to 690 ± 65 nm, respectively. Conversely, CeO_2 and Mn_3O_4 NPs disaggregated in RE over time, decreasing from 289 ± 5 nm to 129 ± 10 nm, and from 761 ± 58 nm to 143 ± 18 nm, respectively. Some of the observed disaggregation can be attributed to the presence of organic ligands, such as detected organic acids, in RE. Moreover, the size of the aggregates decreased substantially for both NPs during the first 24 h, indicating that the larger aggregates were likely soft agglomerates, held together by weaker attractive physical interactions such as van-der-Waals or hydrogen bridge forces.[43] Due to this, the size distribution of all NPs in the early period was analyzed via spICP-MS and presented in a following section. However, a period of 5 days was insufficient to reach colloidal stability for all NPs in RE, since they continued to aggregate or disaggregate. Since NPs with potential use as nanoagrochemicals can reach the roots and soil organisms and the size of clusters or aggregates is an important factor in the interaction at the nano/bio interface,[44] it is important characterize the size of the NPs in RE, which is a representative matrix of the intended application, rather than determining their size in DI water. For example, aggregate size has been shown to influence the apoplastic transport of CeO_2[16] and CuO[17] NPs.

In soil leachate (Figure 3C), all the NPs disaggregated over 5 days. Similar to the results in RE, the disaggregation was more noticeable in the first 24 h. In general, the rate of disaggregation decreased substantially after 3 days and the size of aggregates generally stabilized after that time. However, in the case of $Cu(OH)_2$ and MoO_3 NPs, more time would be needed to reach colloidal stability of the systems. The availability of organic ligands in soil leachate that can be adsorbed onto particle surfaces likely interferes with the weak aggregation, providing a barrier to aggregation.

Dissolution of Metal Oxide Nanoparticles in RE and Soil Leachate. Within the first 6 days of exposure in DI water, CeO_2 NPs did not release ions and the Mn_3O_4 NPs presented an ion release rate of only 0.016%/h of their metal content (Figure 4). However, the $Cu(OH)_2$ nanowires and MoO_3 NPs presented immediate dissolution (t = 0 h) of 5.2% and 34.9%, with rate of 0.072%/h and 0.026%/h thereafter, respectively. In the presence of RE, CeO_2 NPs still did not dissolve in 6 days, while Mn_3O_4 released 0.002%/h after this time. In RE, $Cu(OH)_2$ had an early dissolution of 1% and then a slow rate of 0.001%/h. MoO_3 NPs were the only ones that dissolved nearly as much in DI water as in RE, with an immediate dissolution of 31.3% and 0.047%/h thereafter. While the change was minor for Mn_3O_4, the decrease in overall dissolution for $Cu(OH)_2$ is likely due to pH increase of 0.3 units compared to the DI water, which reduced dissolution 5-fold at a pH of 6.8. The higher pH of RE and soil leachate also decreased the immediate dissolution of MoO_3 NPs and Mn_3O_4 NPs. Similar to the other matrices and in line with previous studies,[16,45] CeO_2 NPs did not release ions in soil leachate either, while $Cu(OH)_2$ and Mn_3O_4 presented an ion release rate <0.001%/h, with a low early dissolution. Conversely, MoO_3 NPs in soil leachate presented an immediate dissolution of 33.7% and the largest ion releasing rate of whole experiment with 0.154%/h.

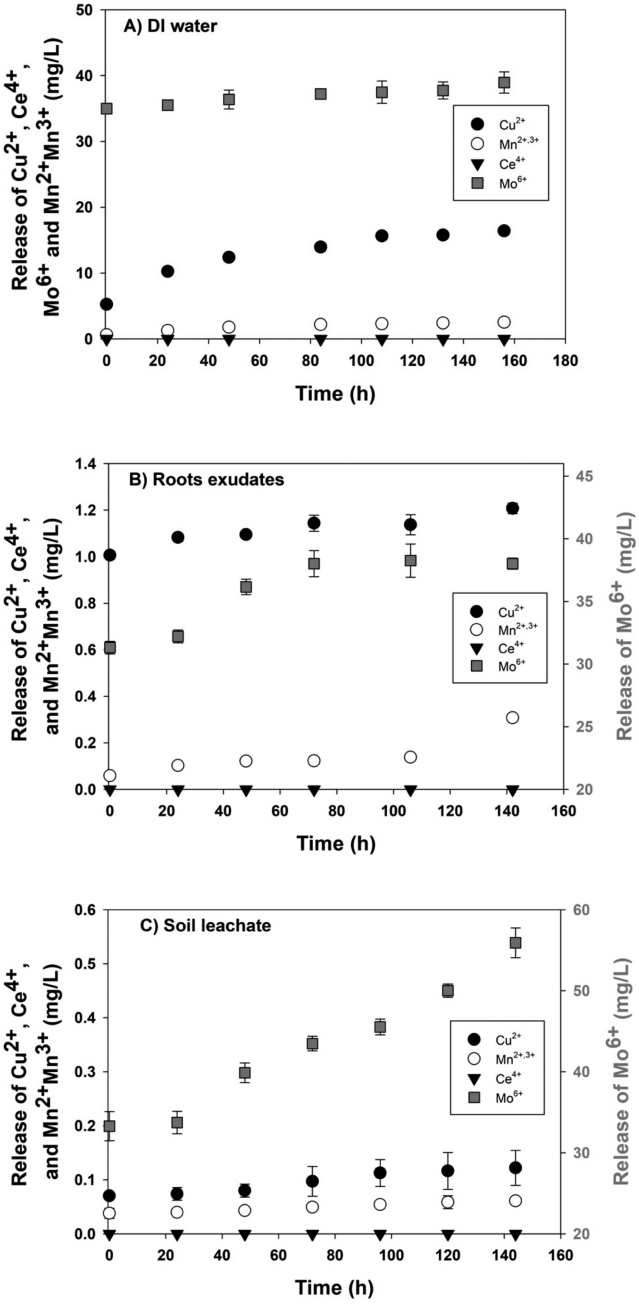

Figure 4. Ions released from CeO_2, Mn_3O_4, $Cu(OH)_2$, and MoO_3 nanoparticles in (A) DI water: (B) RE; and (C) soil leachate. Error bars represent ± standard deviation of triplicate samples (n = 3).

According to the results, the dissolution of NPs in RE was higher than in soil leachate, except for MoO_3 NPs. However, the dissolution rate in both RE and soil leachate was $MoO_3 \gg Cu(OH)_2 > Mn_3O_4 > CeO_2$. Thus, $Cu(OH)_2$, Mn_3O_4, and CeO_2 NPs will exhibit minor dissolution in contact with RE and soil leachate. However, for MoO_3 NPs the formation of more stable chemical forms from the ionized fraction could be feasible. Hence, application of Mo-based NPs into the root-soil interface can result in the environmental buildup of Mo ions or more stable chemical species. Given the low dissolution rate for CeO_2 and Mn_3O_4NPs, this is not likely the main factor in their disaggregation in RE or soil leachate, which can be attributed to the organic ligands present in both media. Given the low dissolution in RE and soil leachate, $Cu(OH)_2$, Mn_3O_4

https://doi.org/10.1021/acs.est.1c00767
Environ. Sci. Technol. XXXX, XXX, XXX−XXX

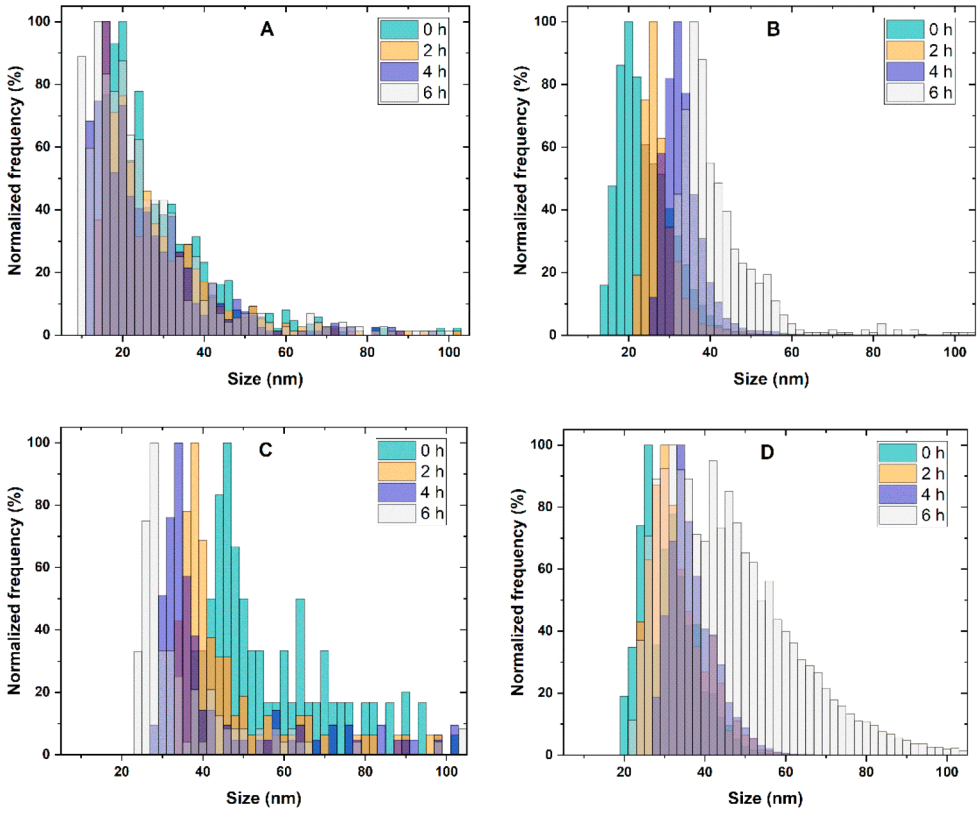

Figure 5. Changes in the size distribution of metal oxide nanoparticles: (A) CeO_2, (B) $Cu(OH)_2$, (C) Mn_3O_4, and (D) MoO_3 during first 6 h in RE.

and CeO_2 NPs may be internalized as NPs up into the endodermis or pericycle, where the chemical environment may favor their dissolution.

Size Distribution of Metal Oxide Nanoparticles in RE. The size distribution of these NPs in RE was measured via spICP-MS for 6 h, at 2 h intervals (Figure 5). For CeO_2 NPs, although the change in size distribution was not as substantial as for the other NPs, there was a clear shift to smaller sizes after first 6 h compared to immediately after spiking (0 h), with single particles as small as 9 nm (Figure 5A). For Mn_3O_4 NPs, the shift to smaller sizes was more significant, and the size distribution became narrower with time (Figure 5C). Conversely, for $Cu(OH)_2$ NPs the size distribution shifted to larger particles with time, and the distribution broadened (Figure 5B) and became multimodal. For MoO_3 NPs the mean size increased over time, and the size distribution became wider with time, but the shape of the distribution was similar to the original one at spiking. It is important to note that for the spICP-MS analysis, the shape of the NPs was assumed to be spherical, since that is the only option in the current algorithm.

Disaggregation in the presence of soybean RE occurred in NPs with low rates of dissolution: CeO_2 and Mn_3O_4 NPs. The spICP-MS size distributions correlated well with the observed decrease in aggregate size of these NPs in RE as measured by the Zetasizer (Figure 3b). This can be attributed to the binding of negatively charged organic acids, which can interfere with the weak attractive forces.[33,35,46] In addition, this is the first time that Mn_3O_4 NPs stability in soil leachate and RE is reported; presenting low rates of dissolution and smaller aggregates size over time in both media.

Conversely, the growth of the aggregates of MoO_3 and $Cu(OH)_2$ NPs observed in the presence of RE correlated with higher dissolution rates and may reflect stronger attractive forces between NPs even in the presence of the organic ligands, or possible bridging between organic molecules.[41,47] Nevertheless, the change in size distributions observed with spICP-MS are in line with the Zetasizer observations. Higher dissolution and nonaggregation of Cu-based NP have been reported for wheat plants in saturated paste extracts,[18] as well as in wheat RE.[19] In both studies, the influence of electrolytes (3.34 mM of $Ca(NO_3)_2$) and organic matter content (up to 305 mg/L of DOC), contributed to the dissolution and nonaggregation of Cu based NPs. This is also in line with previous finding that support that organic matter in soil solution highly correlated with dissolved Cu.[48] Since in our experiment the Cu-based NPs were in contact with low concentration of both electrolyte (0.1 mM of $CaCl_2$) and organic acids, that can also explain the formation of aggregates and low dissolution rate.

While the characterization of NPs in DI water is useful for understanding their general behavior, it can lead to significant misconceptions of how the NPs will actually behave in realistic conditions. Here we demonstrated that the surface charge, aggregation state, size distribution, and amount of metal ion release differed considerably depending on the composition of the aqueous medium into which the NPs are placed. In DI water, all the NPs aggregated, and that influenced the size distribution and the release of metal ions. However, when placed in RE or soil leachate, the aggregation behavior differed substantially from that in DI water, with considerable reversal and disaggregation of all NPs in soil leachate and the CeO_2 and Mn_3O_4 NPs in RE. This was further confirmed by spICP-MS,

https://doi.org/10.1021/acs.est.1c00767
Environ. Sci. Technol. XXXX, XXX, XXX−XXX

which demonstrated the change in particle size distribution, even after just a few hours of exposure of the CeO_2 and Mn_3O_4 NPs to soybean RE. While the rate of release of metal ions in different media did not vary as much for some NPs (i.e., CeO_2, Mn_3O_4, and MoO_3), it was very important for $Cu(OH)_2$NPs, which would result in lower concentrations of ionic or complexed Cu in RE and soil leachate. Therefore, if the dissolution behavior in DI water was used to estimate the exposure concentration of the metal ion in a soil or hydroponic experiment, it could lead to a substantial error.

These results highlight the importance of characterizing the NPs in the exposure medium to be used in subsequent plant exposure experiments, as well as for the design of better delivery mechanisms for the NPs or the active ingredients that they will release. Characterization should include extensive analyses of the main components of an agricultural setting, such as soil and exudates, in terms of the electrolytes, organic matter concentration, identification of main organic molecules in organic matter, pH, and soil cation exchange capacity. A better understanding of the role these factors play will enhance the effectiveness of NP delivery systems at the root-soil interface.

■ ASSOCIATED CONTENT

Supporting Information

The Supporting Information is available free of charge at https://pubs.acs.org/doi/10.1021/acs.est.1c00767.

The operating parameters of the instrument for single particle ICP-MS analysis and the graphs of LSPR, XPS, and XRD for all four NPs are presented in one table and four figures (PDF)

■ AUTHOR INFORMATION

Corresponding Author

Arturo A. Keller − *Bren School of Environmental Science and Management, University of California at Santa Barbara, Santa Barbara, California 93106, United States; University of California, Center for Environmental Implications of Nanotechnology, Santa Barbara, California 93106, United States;* orcid.org/0000-0002-7638-662X; Phone: +1 805 893 7548; Email: keller@bren.ucsb.edu; Fax: +1 805 893 7612

Authors

Pabel Cervantes-Avilés − *Tecnológico de Monterrey, Escuela de Ingeniería y Ciencias, Reserva Territorial Atlixcáyotl, Puebla, CP 72453, México; University of California, Center for Environmental Implications of Nanotechnology, Santa Barbara, California 93106, United States;* orcid.org/0000-0001-9665-2959

Xiangning Huang − *Bren School of Environmental Science and Management, University of California at Santa Barbara, Santa Barbara, California 93106, United States*

Complete contact information is available at: https://pubs.acs.org/10.1021/acs.est.1c00767

Notes

The authors declare no competing financial interest.

■ ACKNOWLEDGMENTS

This work was supported by the National Science Foundation (NSF) under cooperative agreement number NSF-1901515. Arturo A. Keller also appreciates Agilent Technologies for their Agilent Thought Leader Award. Pabel Cervantes-Aviles thanks CONACYT.

■ REFERENCES

(1) Wu, L.; Zhu, H.; Chen, H.; Roco, M. C. Comparing Nanotechnology Landscapes in the US and China: A Patent Analysis Perspective. *J. Nanopart. Res.* **2019**, *21* (8). DOI: 10.1007/s11051-019-4608-0.

(2) Lowry, G. V.; Avellan, A.; Gilbertson, L. M. Opportunities and Challenges for Nanotechnology in the Agri-Tech Revolution. *Nat. Nanotechnol.* **2019**, *14* (6), 517−522.

(3) Giraldo, J. P.; Wu, H.; Newkirk, G. M.; Kruss, S. Nanobiotechnology Approaches for Engineering Smart Plant Sensors. *Nat. Nanotechnol.* **2019**, *14* (6), 541−553.

(4) Wang, Z.; Yue, L.; Dhankher, O. P.; Xing, B. Nano-Enabled Improvements of Growth and Nutritional Quality in Food Plants Driven by Rhizosphere Processes. *Environ. Int.* **2020**, *142* (May), 105831.

(5) Gomez, A.; Narayan, M.; Zhao, L.; Jia, X.; Bernal, R. A.; Lopez-Moreno, M. L.; Peralta-Videa, J. R. Effects of Nano-Enabled Agricultural Strategies on Food Quality: Current Knowledge and Future Research Needs. *J. Hazard. Mater.* **2021**, *401* (July 2020), 123385.

(6) Kah, M.; Hofmann, T. Nanopesticide Research: Current Trends and Future Priorities. *Environ. Int.* **2014**, *63*, 224−235.

(7) Majumdar, S.; Keller, A. A. Omics to Address the Opportunities and Challenges of Nanotechnology in Agriculture. *Crit. Rev. Environ. Sci. Technol.* **2020**, *0* (0), 1−42.

(8) Yin, J.; Wang, Y.; Gilbertson, L. M. Opportunities to Advance Sustainable Design of Nano-Enabled Agriculture Identified through a Literature Review. *Environ. Sci.: Nano* **2018**, *5* (1), 11−26.

(9) Pourzahedi, L.; Pandorf, M.; Ravikumar, D.; Zimmerman, J. B.; Seager, T. P.; Theis, T. L.; Westerhoff, P.; Gilbertson, L. M.; Lowry, G. V. Life Cycle Considerations of Nano-Enabled Agrochemicals: Are Today's Tools up to the Task? *Environ. Sci.: Nano* **2018**, *5* (5), 1057−1069.

(10) Su, Y.; Ashworth, V.; Kim, C.; Adeleye, A. S.; Rolshausen, P.; Roper, C.; White, J.; Jassby, D. Delivery, Uptake, Fate, and Transport of Engineered Nanoparticles in Plants: A Critical Review and Data Analysis. *Environ. Sci.: Nano* **2019**, *6* (8), 2311−2331.

(11) Adisa, I. O.; Pullagurala, V. L. R.; Peralta-Videa, J. R.; Dimkpa, C. O.; Elmer, W. H.; Gardea-Torresdey, J. L.; White, J. C. Recent Advances in Nano-Enabled Fertilizers and Pesticides: A Critical Review of Mechanisms of Action. *Environ. Sci.: Nano* **2019**, *6* (7), 2002−2030.

(12) Schwab, F.; Zhai, G.; Kern, M.; Turner, A.; Schnoor, J. L.; Wiesner, M. R. Barriers, Pathways and Processes for Uptake, Translocation and Accumulation of Nanomaterials in Plants − Critical Review. *Nanotoxicology* **2016**, *10* (3), 1−22.

(13) Lv, J.; Christie, P.; Zhang, S. Uptake, Translocation, and Transformation of Metal-Based Nanoparticles in Plants: Recent Advances and Methodological Challenges. *Environ. Sci.: Nano* **2019**, *6* (1), 41−59.

(14) Huang, Y.; Zhao, L.; Keller, A. A. Interactions, Transformations, and Bioavailability of Nano-Copper Exposed to Root Exudates. *Environ. Sci. Technol.* **2017**, *51* (17), 9774−9783.

(15) Li, J.; Tappero, R. V.; Acerbo, A. S.; Yan, H.; Chu, Y.; Lowry, G. V.; Unrine, J. M. Effect of CeO 2 Nanomaterial Surface Functional Groups on Tissue and Subcellular Distribution of Ce in Tomato (Solanum Lycopersicum). *Environ. Sci.: Nano* **2019**, *6* (1), 273−285.

(16) Zhao, L.; Peralta-Videa, J. R.; Varela-Ramirez, A.; Castillo-Michel, H.; Li, C.; Zhang, J.; Aguilera, R. J.; Keller, A. A.; Gardea-Torresdey, J. L. Effect of Surface Coating and Organic Matter on the Uptake of CeO 2 NPs by Corn Plants Grown in Soil: Insight into the Uptake Mechanism. *J. Hazard. Mater.* **2012**, *225−226*, 131−138.

(17) Wang, Z.; Xie, X.; Zhao, J.; Liu, X.; Feng, W.; White, J. C.; Xing, B. Xylem- and Phloem-Based Transport of CuO Nanoparticles

in Maize (Zea Mays L.). *Environ. Sci. Technol.* **2012**, *46* (8), 4434−4441.
(18) Hortin, J. M.; Anderson, A. J.; Britt, D. W.; Jacobson, A. R.; McLean, J. E. Copper Oxide Nanoparticle Dissolution at Alkaline PH Is Controlled by Dissolved Organic Matter: Influence of Soil-Derived Organic Matter, Wheat, Bacteria, and Nanoparticle Coating. *Environ. Sci.: Nano* **2020**, *7* (9), 2618−2631.
(19) Hortin, J. M.; Anderson, A. J.; Britt, D. W.; Jacobson, A. R.; McLean, J. E. Soil-Derived Fulvic Acid and Root Exudates, Modified by Soil Bacteria, Alter CuO Nanoparticle-Induced Root Stunting of Wheat: Via Cu Complexation. *Environ. Sci.: Nano* **2019**, *6* (12), 3638−3652.
(20) Osman, S. A.; Salama, D. M.; Abd El-Aziz, M. E.; Shaaban, E. A.; Abd Elwahed, M. S. The Influence of MoO3-NPs on Agro-Morphological Criteria, Genomic Stability of DNA, Biochemical Assay, and Production of Common Dry Bean (Phaseolus Vulgaris L.). *Plant Physiol. Biochem.* **2020**, *151* (January), 77−87.
(21) Taran, N. Y.; Gonchar, O. M.; Lopatko, K. G.; Batsmanova, L. M.; Patyka, M. V.; Volkogon, M. V. The Effect of Colloidal Solution of Molybdenum Nanoparticles on the Microbial Composition in Rhizosphere of Cicer Arietinum L. *Nanoscale Res. Lett.* **2014**, *9* (1), 1−8.
(22) Pradhan, S.; Patra, P.; Mitra, S.; Dey, K. K.; Jain, S.; Sarkar, S.; Roy, S.; Palit, P.; Goswami, A. Manganese Nanoparticles: Impact on Non-Nodulated Plant as a Potent Enhancer in Nitrogen Metabolism and Toxicity Study Both in Vivo and in Vitro. *J. Agric. Food Chem.* **2014**, *62* (35), 8777−8785.
(23) Shebl, A.; Hassan, A. A.; Salama, D. M.; Abd El-Aziz, M. E.; Abd Elwahed, M. S. A. Green Synthesis of Nanofertilizers and Their Application as a Foliar for Cucurbita Pepo L. *J. Nanomater.* **2019** *2019*. 1.
(24) Dimkpa, C. O.; Singh, U.; Adisa, I. O.; Bindraban, P. S.; Elmer, W. H.; Gardea-Torresdey, J. L.; White, J. C. Effects of Manganese Nanoparticle Exposure on Nutrient Acquisition in Wheat (Triticum Aestivum L.). *Agronomy* **2018**, *8* (9), 1−16.
(25) Zhao, L.; Huang, Y.; Hu, J.; Zhou, H.; Adeleye, A. S.; Keller, A. A. 1H NMR and GC-MS Based Metabolomics Reveal Defense and Detoxification Mechanism of Cucumber Plant under Nano-Cu Stress. *Environ. Sci. Technol.* **2016**, *50* (4), 2000−2010.
(26) Anumol, T.; Zhao, L.; Huang, Y.; Keller, A. A.; Minakova, A. S.; Adeleye, A. S. Antioxidant Response of Cucumber (Cucumis Sativus) Exposed to Nano Copper Pesticide: Quantitative Determination via LC-MS/MS. *Food Chem.* **2019**, *270* (May 2018), 47−52.
(27) Montaño, M. D.; Badiei, H. R.; Bazargan, S.; Ranville, J. F. Improvements in the Detection and Characterization of Engineered Nanoparticles Using SpICP-MS with Microsecond Dwell Times. *Environ. Sci.: Nano* **2014**, *1* (4), 338−346.
(28) Pace, H. E.; Rogers, N. J.; Jarolimek, C.; Coleman, V. A.; Higgins, C. P.; Ranville, J. F. Determining Transport Efficiency for the Purpose of Counting and Sizing Nanoparticles via Single Particle Inductively Coupled Plasma Mass Spectrometry. *Anal. Chem.* **2011**, *83* (24), 9361−9369.
(29) Cervantes-Avilés, P.; Keller, A. A. Incidence of Metal-Based Nanoparticles in the Conventional Wastewater Treatment Process. *Water Res.* **2021**, *189*, 189.
(30) Laborda, F.; Bolea, E.; Jiménez-Lamana, J. Single Particle Inductively Coupled Plasma Mass Spectrometry: A Powerful Tool for Nanoanalysis. *Anal. Chem.* **2014**, *86* (5), 2270−2278.
(31) Huang, Y.; Keller, A. A.; Cervantes-Avilés, P.; Nelson, J. Fast Multielement Quantification of Nanoparticles in Wastewater and Sludge Using Single-Particle ICP-MS. *ACS ES&T Water* **2021**, *1*205.
(32) Dupin, J. C.; Gonbeau, D.; Vinatier, P.; Levasseur, A. Systematic XPS Studies of Metal Oxides, Hydroxides and Peroxides. *Phys. Chem. Chem. Phys.* **2000**, *2* (6), 1319−1324.
(33) Rossi, L.; Sharifan, H.; Zhang, W.; Schwab, A. P.; Ma, X. Mutual Effects and: In Planta Accumulation of Co-Existing Cerium Oxide Nanoparticles and Cadmium in Hydroponically Grown Soybean (Glycine Max (L.) Merr.). *Environ. Sci.: Nano* **2018**, *5* (1), 150−157.
(34) Araújo, M. P.; Nunes, M.; Rocha, I. M.; Pereira, M. F. R.; Freire, C. Electrocatalytic Activity of New Mn 3 O 4 @oxidized Graphene Flakes Nanocomposites toward Oxygen Reduction Reaction. *J. Mater. Sci.* **2019**, *54* (12), 8919−8940.
(35) Huang, Y.; Zhao, L.; Keller, A. A. Interactions, Transformations, and Bioavailability of Nano-Copper Exposed to Root Exudates. *Environ. Sci. Technol.* **2017**, *51* (17), 9774−9783.
(36) Zhan, Y.; Liu, Y.; Zu, H.; Guo, Y.; Wu, S.; Yang, H.; Liu, Z.; Lei, B.; Zhuang, J.; Zhang, X.; Huang, D.; Hu, C. Phase-Controlled Synthesis of Molybdenum Oxide Nanoparticles for Surface Enhanced Raman Scattering and Photothermal Therapy. *Nanoscale* **2018**, *10* (13), 5997−6004.
(37) Gu, H.; Soucek, M. D. Preparation and Characterization of Monodisperse Cerium Oxide Nanoparticles in Hydrocarbon Solvents. *Chem. Mater.* **2007**, *19* (5), 1103−1110.
(38) Garcês Gonçalves, P. R.; De Abreu, H. A.; Duarte, H. A. Stability, Structural, and Electronic Properties of Hausmannite (Mn3O4) Surfaces and Their Interaction with Water. *J. Phys. Chem. C* **2018**, *122* (36), 20841−20849.
(39) Keller, A. A.; Wang, H.; Zhou, D.; Lenihan, H. S.; Cherr, G.; Cardinale, B. J.; Miller, R.; Ji, Z. Stability and Aggregation of Metal Oxide Nanoparticles in Natural Aqueous Matrices. *Environ. Sci. Technol.* **2010**, *44* (6), 1962−1967.
(40) Tombácz, E.; Tóth, I. Y.; Nesztor, D.; Illés, E.; Hajdú, A.; Szekeres, M.; Vékás, L. Adsorption of Organic Acids on Magnetite Nanoparticles, PH-Dependent Colloidal Stability and Salt Tolerance. *Colloids Surf., A* **2013**, *435*, 91−96.
(41) Chen, H. Metal Based Nanoparticles in Agricultural System: Behavior, Transport, and Interaction with Plants. *Chem. Speciation Bioavailability* **2018**, *30* (1), 123−134.
(42) Ma, Y.; He, X.; Zhang, P.; Zhang, Z.; Guo, Z.; Tai, R.; Xu, Z.; Zhang, L.; Ding, Y.; Zhao, Y.; Chai, Z. Phytotoxicity and Biotransformation of La $_2$ O $_3$ Nanoparticles in a Terrestrial Plant Cucumber (*Cucumis Sativus*). *Nanotoxicology* **2011**, *5* (4), 743−753.
(43) Teleki, A.; Wengeler, R.; Wengeler, L.; Nirschl, H.; Pratsinis, S. E. Distinguishing between Aggregates and Agglomerates of Flame-Made TiO2 by High-Pressure Dispersion. *Powder Technol.* **2008**, *181* (3), 292−300.
(44) Aubert, T.; Burel, A.; Esnault, M. A.; Cordier, S.; Grasset, F.; Cabello-Hurtado, F. Root Uptake and Phytotoxicity of Nanosized Molybdenum Octahedral Clusters. *J. Hazard. Mater.* **2012**, *219*−*220*, 111−118.
(45) Conway, J. R.; Hanna, S. K.; Lenihan, H. S.; Keller, A. A. Effects and Implications of Trophic Transfer and Accumulation of CeO 2 Nanoparticles in a Marine Mussel. *Environ. Sci. Technol.* **2014**, *48* (3), 1517−1524.
(46) Rico, C. M.; Johnson, M. G.; Marcus, M. A. Cerium Oxide Nanoparticles Transformation at the Root-Soil Interface of Barley (Hordeum Vulgare L.). *Environ. Sci.: Nano* **2018**, *5* (8), 1807−1812.
(47) Auvinen, H.; Gagnon, V.; Rousseau, D. P. L.; Du Laing, G. Fate of Metallic Engineered Nanomaterials in Constructed Wetlands: Prospection and Future Research Perspectives. *Rev. Environ. Sci. Bio/Technol.* **2017**, *16* (2), 207−222.
(48) Gao, X.; Rodrigues, S. M.; Spielman-Sun, E.; Lopes, S.; Rodrigues, S.; Zhang, Y.; Avellan, A.; Duarte, R. M. B. O.; Duarte, A.; Casman, E. A.; Lowry, G. V. Effect of Soil Organic Matter, Soil PH, and Moisture Content on Solubility and Dissolution Rate of CuO NPs in Soil. *Environ. Sci. Technol.* **2019**, *53* (9), 4959−4967.

https://doi.org/10.1021/acs.est.1c00767
Environ. Sci. Technol. XXXX, XXX, XXX−XXX